Acta Mech 208, 11–26 (2009)
DOI 10.1007/s00707-008-0114-7

P. J. Lin · J. W. Ju

Effective elastic moduli of three-phase composites with randomly located and interacting spherical particles of distinct properties

Received: 28 July 2008 / Published online: 27 November 2008

Abstract A micromechanical analytical framework is presented to predict effective elastic moduli of three-phase composites containing many randomly dispersed and pairwisely interacting spherical particles. Specifically, the two inhomogeneity phases feature *distinct* elastic properties. A higher-order structure is proposed based on the probabilistic spatial distribution of spherical particles, the pairwise particle interactions, and the ensemble-volume homogenization method. Two non-equivalent formulations are considered in detail to derive effective elastic moduli with heterogeneous inclusions. As a special case, the effective shear modulus for an incompressible matrix containing randomly dispersed and identical rigid spheres is derived. It is demonstrated that a significant improvement in the singular problem and accuracy is achieved by employing the proposed methodology. Comparisons among our theoretical predictions, available experimental data, and other analytical predictions are rendered. Moreover, numerical examples are implemented to illustrate the potential of the present method.

1 Introduction

Composite materials have developed rapidly over the last several decades to meet the diverse needs for improved material performance with enhanced thermo-mechanical properties, reduced unit weights, versatile directionality, optimal anisotropy, as well as improvements in mechanical strengths, elastic moduli, delamination resistance, fracture toughness and fatigue resistance, etc. Reinforcements could be continuous in the form of fibers, or discontinuous in the form of particles or whiskers. In particular, the prediction and estimation of overall mechanical properties of random heterogeneous multiphase composites are of considerable interest to engineers in many science and engineering disciplines. In general, mechanical properties of composites are related to properties of constituent phases and microstructures of inhomogeneities (e.g., the shapes, orientations, aspect ratios, volume fractions, and random locations).

Many studies have been published in the literature for predicting effective elastic moduli of particle reinforced composites. For example, we refer to Hashin and Shtrikman [1–3], Torquato and Lado [4], Mori and Tanaka [5], Sen et al. [6], Nemat-Nasser and Hori [7], Eshelby [8], and Batchelor and Green [9] for select literature reviews. Specifically, Hashin and Shtrikman [1–3] proposed the upper and lower bounds for effective elastic moduli of multiphase materials. Their method was based on the variational principles within the linear elasticity theory. Their method renders generally better bounds than the Voigt and Reuss bounds. The

P. J. Lin
Department of Construction Technology, Tungnan University, Taipei, Taiwan

J. W. Ju (✉)
Department of Civil and Environmental Engineering, University of California, Los Angeles, CA 90095-1593, USA
E-mail: juj@ucla.edu
URL: http://www.cee.ucla.edu/faculty/ju.htm

"improved" higher-order mathematical bounds (which depend on the statistical microstructural information of random heterogeneous composites) were also investigated by Silnutzer [10], Milton and Phan-Thien [11], Torquato and Lado [4], Sen et al. [6], etc. Further, effective elastic moduli of composites were studied by using the "effective medium methods" such as the self-consistent method, the differential scheme, the generalized self-consistent method, and the Mori–Tanaka method [5]. However, the effective medium methods as a group depend only on geometries of particles (inclusions) and volume fractions; they do not consider the spatial locations or probabilistic distributions of particles (inclusions). The effective medium methods are inherently independent of the spatial or statistical particle distributions, thus best suited for low particle concentrations or some limited special configurations. In contrast, microstructure-dependent particle interaction methods were proposed in the literature to predict effective elastic properties of composites with spatially randomly located yet locally interacting inclusions by employing micromechanical approximations, or by featuring special configurations for inclusions dispersed in the matrix; see, e.g., Batchelor and Green [9], and Chen and Acrivos [12].

In Ju and Chen [13,14], a novel higher-order (in $\boldsymbol{\phi}$) ensemble-volume micromechanical framework was presented to predict effective elastic moduli of multi-phase composites containing randomly dispersed identical spherical or ellipsoidal inhomogeneities. Explicit probabilistic micromechanical pairwise inter-particle interactions were accounted for during the derivations of effective elastic moduli in Ju and Chen [13,14]. Moreover, the ensemble-volume homogenization procedure was utilized, and the formulation was of complete second order. Ju and Chen showed that effective elastic properties predicted by the Mori–Tanaka method [5] coincide with their first-order results and Hashin–Shtrikman [3] bounds for isotropic composites, and with Wills [15] bounds for anisotropic composites containing unidirectionally aligned and identically shaped inclusions. Emanating from the general framework of Ju and Chen [13,14], Ju and co-workers further investigated the micromechanics and effective elastoplastic behaviors of two-phase metal matrix composites [16–20], micromechanical effective transverse elastic moduli and elastoplastic behaviors of composites with randomly located yet aligned circular fibers [21,22], the exact formulation for the exterior-point Eshelby's tensor of an ellipsoidal inclusion [23], and micromechanical damage models for effective elastoplastic behaviors of ductile matrix composites accommodating evolutionary particle debonding and cracking [24–30] or progressive interfacial fiber debonding [31–34].

The primary objective of the present paper is to extend the framework of Ju and Chen [13,14] to predict effective elastic moduli of three-phase composites based on mechanical properties of the constituent phases, volume fractions, spatial distributions of particles, and direct inter-particle interactions. The two inclusion phases feature distinct elastic properties. All particles are considered non-intersecting, randomly dispersed, and embedded firmly in the matrix with perfect interfaces. A higher-order framework is constructed based on the probabilistic spatial distribution of spherical particles, pairwise particle interactions, and the ensemble-volume averaging procedure for three-phase elastic composites.

The remainder of the paper is organized as follows. In Sect. 2, we present the approximate analytical solutions for the direct interactions between two different, randomly located elastic spheres embedded in the matrix material. Subsequently, the ensemble-volume averaged eigenstrains are obtained through the probabilistic pairwise particle interaction mechanism. Two non-equivalent formulations are considered in detail to derive effective elastic moduli of three-phase composites. In combination with the results from Sect. 2 and the governing ensemble-volume averaged field equations, effective elastic moduli of three-phase composites containing randomly dispersed distinct spherical particles are analytically derived in Sect. 3. Comparisons between our micromechanical predictions and other homogenization methods as well as experimental data are rendered in Sect. 4. As a special case, a three-phase composite containing randomly dispersed microvoids and rigid spheres embedded in an elastic matrix is also considered.

2 Approximate local solutions of two interacting particles

Let us consider a three-phase composite consisting of an isotropic elastic matrix (phase 0) with the bulk modulus κ_0 and shear modulus μ_0, randomly dispersed elastic spherical particles (phase 1) with the bulk modulus κ_1 and shear modulus μ_1, and randomly dispersed elastic spherical particles (phase 2) with the bulk modulus κ_2 and shear modulus μ_2 (cf. Fig. 1). In addition, the linearly elastic isotropic stiffness tensors for three distinct phases are expressed as

$$(C_\eta)_{ijkl} = \lambda_\eta\, \delta_{ij}\, \delta_{kl} + \mu_\eta\, (\delta_{ik}\delta_{jl} + \delta_{il}\delta_{jk}), \quad \eta = 0, 1, 2, \tag{1}$$

where λ_η and μ_η are the Lamé constants of the phase-η material.

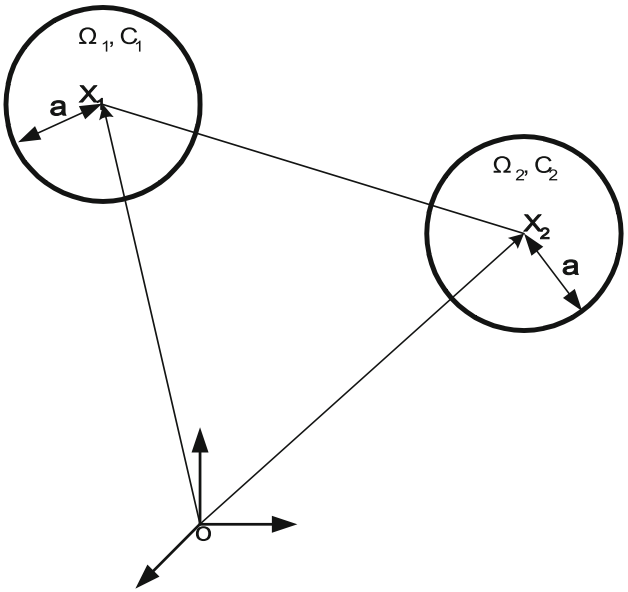

Fig. 1 The schematic diagram for the two-particle interaction problem

Following the eigenstrain concept introduced by Eshelby [8,35], the perturbed strain field $\boldsymbol{\varepsilon}'(x)$ induced by particles can be related to the specified eigenstrains $\boldsymbol{\varepsilon}^*(x)$ by replacing the particles with the matrix material. The key equation can be rephrased as follows:

$$\mathbf{C}_{\eta} : [\boldsymbol{\varepsilon}^0 + \boldsymbol{\varepsilon}'(\mathbf{x})] = \mathbf{C}_0 : [\boldsymbol{\varepsilon}^0 + \boldsymbol{\varepsilon}'(\mathbf{x}) - \boldsymbol{\varepsilon}^*(\mathbf{x})], \quad \eta = 1, 2, \tag{2}$$

where $\boldsymbol{\varepsilon}^0$ is the uniform strain field induced by the far-field loads for a homogeneous matrix material only. Throughout the paper, the colon symbol "**:**" denotes the tensor contraction between a fourth-rank tensor and a second-rank tensor, while the dot symbol "•" represents the tensor multiplication between two four-rank tensors.

According to Eshelby [8,35], the perturbed strain field induced by the distributed eigenstrain $\boldsymbol{\varepsilon}^*(x)$ in a representative volume element (RVE) V reads

$$\boldsymbol{\varepsilon}'(x) = \int_V \mathbf{G}(\mathbf{x} - \mathbf{x}') : \boldsymbol{\varepsilon}^*(\mathbf{x}')\, \mathbf{d}\mathbf{x}', \tag{3}$$

where $\mathbf{x}, \mathbf{x}' \in V$ and the components of the fourth-rank three-dimensional Green's function tensor $\mathbf{G}$ take the form

$$G_{ijkl}(\mathbf{x} - \mathbf{x}') = \frac{1}{8\,\pi(1-\nu_0)r^3}\, F_{ijkl}(-15,\ 3\nu_0,\ 3,\ 3-6\nu_0, -1+2\nu_0,\ 1-2\nu_0), \tag{4}$$

where $i, j, k, l = 1, 2, 3$ (cf. Mura [36]), $\mathbf{r} = \mathbf{x} - \mathbf{x}'$ and $r = \|\mathbf{x} - \mathbf{x}'\|$. The components of the tensor $\boldsymbol{F}$ – which depends on its arguments $(B_1, B_2, B_3, B_4, B_5, B_6)$ – are defined by ($m = 1$ to 6):

$$\begin{aligned} F_{ijkl}(B_m) \equiv\ & B_1\, n'_i n'_j n'_k n'_l + B_2\, (\delta_{ik} n'_j n'_l + \delta_{il} n'_j n'_k + \delta_{jk} n'_i n'_l + \delta_{jl} n'_i n'_k) \\ & + B_3\, \delta_{ij} n'_k n'_l + B_4\, \delta_{kl} n'_i n'_j + B_5\, \delta_{ij}\delta_{kl} + B_6\, (\delta_{ik}\delta_{jl} + \delta_{il}\delta_{jk}) \end{aligned} \tag{5}$$

with the normal vector $\boldsymbol{n}' \equiv \mathbf{r}/r$. All physical quantities refer to the Cartesian coordinates, and the summation convention applies here. Furthermore, δ_{ij} is the Kronecker delta, and ν_0 defines the Poisson's ratio of the homogeneous matrix.

From Eqs. (2) and (3), we arrive at

$$-\mathbf{A}_i : \boldsymbol{\varepsilon}^*(\boldsymbol{x}) = \boldsymbol{\varepsilon}^0 + \int_V \mathbf{G}(\mathbf{x} - \mathbf{x}') : \boldsymbol{\varepsilon}^*(\mathbf{x}')\, \mathbf{d}\mathbf{x}' \tag{6}$$

for $\mathbf{x} \in V$, and

$$\mathbf{A}_i \equiv (\mathbf{C}_i - \mathbf{C}_0)^{-1} \bullet \mathbf{C}_0. \tag{7}$$

Within the present two-sphere interaction context, the integral Eq. (6) can be recast as

$$-\mathbf{A}_i : \boldsymbol{\varepsilon}^*_{(i)}(\mathbf{x}) = \boldsymbol{\varepsilon}^0 + \int_{\Omega_i} \mathbf{G}(\mathbf{x} - \mathbf{x}') : \boldsymbol{\varepsilon}^*_{(i)}(\mathbf{x}')\, \mathbf{dx}' + \int_{\Omega_j} \mathbf{G}(\mathbf{x} - \mathbf{x}') : \boldsymbol{\varepsilon}^*_{(j)}(\mathbf{x}')\, \mathbf{dx}', \quad i \neq j, \quad i, j = 1, 2, \tag{8}$$

where $\mathbf{x} \in \Omega_i$, and $\boldsymbol{\varepsilon}^*_{(i)}(\mathbf{x}')$ is the eigenstrain at $\mathbf{x}'$ in the ith sphere within the domain Ω_i.

As discussed earlier in Ju and Chen [13], the first-order solution for the eigenstrain, denoted by $\boldsymbol{\varepsilon}^{*0}_{(i)}$ for the ith phase, can be obtained by neglecting the last term in the right-hand side of Eq. (8), which represents the interaction effects due to the other sphere. The first-order formulation leads to

$$-\mathbf{A}_i : \boldsymbol{\varepsilon}^{*0}_{(i)} = \boldsymbol{\varepsilon}^0 + \mathbf{s} : \boldsymbol{\varepsilon}^{*0}_{(i)}, \tag{9}$$

where the Eshelby tensor $\mathbf{s}$ is defined as

$$\mathbf{s} \equiv \int_{\Omega_i} \mathbf{G}(\mathbf{x} - \mathbf{x}')\, \mathbf{dx}', \qquad \mathbf{x} \in \Omega_i. \tag{10}$$

The components of $\mathbf{s}$ depend on the Poisson's ratio of the matrix (ν_0) and the shape of the particle Ω_i. For a spherical particle, the tensor $\mathbf{s}$ reads

$$s_{ijkl} = \frac{1}{15\,(1-\nu_0)} \left\{ (5\nu_0 - 1)\, \delta_{ij}\delta_{kl} + (4 - 5\nu_0)\, (\delta_{ik}\delta_{jl} + \delta_{il}\delta_{jk}) \right\}. \tag{11}$$

We refer to Mura [36] for more details.

By subtracting the first-order solution Eq. (9) from Eq. (8), the effects of inter-particle interactions can be derived by solving the following integral equation:

$$\begin{aligned} -\mathbf{A}_i : \mathbf{d}^*_{(i)}(\mathbf{x}) = &\int_{\Omega_j} \mathbf{G}(\mathbf{x} - \mathbf{x}')\, \mathbf{dx}' : \boldsymbol{\varepsilon}^{*0}_{(j)} + \int_{\Omega_i} \mathbf{G}(\mathbf{x} - \mathbf{x}') : \mathbf{d}^*_{(i)}(\mathbf{x}')\, \mathbf{dx}' \\ &+ \int_{\Omega_j} \mathbf{G}(\mathbf{x} - \mathbf{x}') : \mathbf{d}^*_{(j)}(\mathbf{x}')\, \mathbf{dx}', \quad \text{for} \quad \mathbf{x} \in \Omega_i, \quad i \neq j, \end{aligned} \tag{12}$$

where

$$\mathbf{d}^*_{(i)}(\mathbf{x}) \equiv \boldsymbol{\varepsilon}^*_{(i)}(\mathbf{x}) - \boldsymbol{\varepsilon}^{*0}_{(i)}. \tag{13}$$

To obtain the higher-order interaction correction for $\boldsymbol{\varepsilon}^*_{(i)}(\mathbf{x})$, one may expand the fourth-rank tensor $\mathbf{G}(\mathbf{x} - \mathbf{x}')$ in the domain Ω_j with respect to its center point $\mathbf{x}$; i.e.,

$$\begin{aligned} \mathbf{G}(\mathbf{x} - \mathbf{x}') = &\mathbf{G}(\mathbf{x} - \mathbf{x}_j) - (\mathbf{x}' - \mathbf{x}_j) : [\nabla_{\mathbf{x}} \otimes \mathbf{G}(\mathbf{x} - \mathbf{x}_j)] \\ &+ \frac{1}{2}[(\mathbf{x}' - \mathbf{x}_j) \otimes (\mathbf{x}' - \mathbf{x}_j)] : [\nabla_{\mathbf{x}} \otimes \nabla_{\mathbf{x}} \otimes \mathbf{G}(\mathbf{x} - \mathbf{x}_j)] + \cdots \end{aligned} \tag{14}$$

where the relation

$$\nabla_{\mathbf{x}'} \otimes \mathbf{G}(\mathbf{x} - \mathbf{x}') = -\nabla_{\mathbf{x}} \otimes \mathbf{G}(\mathbf{x} - \mathbf{x}') \tag{15}$$

has been employed. From Eqs. (12) and (14), we arrive at

$$\begin{aligned} -\mathbf{A}_i : \mathbf{d}^*_{(i)}(\mathbf{x}) = &\int_{\Omega_j} \mathbf{G}(\mathbf{x} - \mathbf{x}')\, \mathbf{dx}' : \boldsymbol{\varepsilon}^{*0}_{(j)} + \int_{\Omega_i} \mathbf{G}(\mathbf{x} - \mathbf{x}') : \mathbf{d}^*_{(i)}(\mathbf{x}')\, \mathbf{dx}' \\ &+ \Omega_j\, \mathbf{G}(\mathbf{x} - \mathbf{x}_j) : \overline{\mathbf{d}}^*_{(j)}(\mathbf{x}_j) \; - \Omega_j a_j\, \{\nabla_{\mathbf{x}} \otimes \mathbf{G}(\mathbf{x} - \mathbf{x}_j)\} : \overline{\mathbf{P}}^*_{(j)} \\ &+ \frac{1}{2}\Omega_j\, a_j^2\, \{\nabla_{\mathbf{x}} \otimes \nabla_{\mathbf{x}} \otimes \mathbf{G}(\mathbf{x} - \mathbf{x}_j)\} : \overline{\mathbf{Q}}^*_{(j)} + \cdots \end{aligned} \tag{16}$$

for $\mathbf{x} \in \Omega_i$ and $i \neq j \ \ (i, j = 1, 2)$. Here $\Omega = \Omega_i = \Omega_j = 4\pi a^3/3$ denotes the volume of a spherical particle, and $a = a_i = a_j$ defines its radius. Moreover, the averaged fields involved in Eq. (16) are defined as follows:

$$\overline{\mathbf{d}}^*_{(j)} \equiv \frac{1}{\Omega_j} \int\limits_{\Omega_j} \mathbf{d}^*_{(j)}(\mathbf{x})\, \mathbf{dx}, \tag{17}$$

$$\overline{\mathbf{P}}^*_{(j)} \equiv \frac{1}{\Omega_j a_j} \int\limits_{\Omega_j} (\mathbf{x} - \mathbf{x}_j) \otimes \mathbf{d}^*_{(j)}(\mathbf{x})\, \mathbf{dx}, \tag{18}$$

$$\overline{\mathbf{Q}}^*_{(j)} \equiv \frac{1}{\Omega_j a_j^2} \int\limits_{\Omega_j} (\mathbf{x} - \mathbf{x}_j) \otimes (\mathbf{x} - \mathbf{x}_j) \otimes \mathbf{d}^*_{(j)}(\mathbf{x})\, \mathbf{dx}. \tag{19}$$

The third-rank tensor $\overline{\mathbf{P}}^*_{(j)}$ and the fourth-rank tensor $\overline{\mathbf{Q}}^*_{(j)}$ correspond to the dipole and quadrapole of $\mathbf{d}^*_{(j)}$ in the domain Ω_j, respectively. Due to the spherical symmetry of particles, the leading order of $\overline{\mathbf{P}}^*_{(j)}$ is of the order $O(\rho^4)$, rather than $O(\rho^3)$, by substituting Eq. (18) into Eq. (16). Here, $\rho \equiv a/r$, and r is the spacing between the centers of two spheres. By performing the volume average in Eq. (16) for the domain Ω_i and truncating those terms of higher order moments, the approximate equations $\overline{\mathbf{d}}^*_{(i)}$ for the local two-sphere interaction problem can be exhibited:

$$-\mathbf{A}_i : \overline{\mathbf{d}}^*_{(i)} = \mathbf{G}^2(\mathbf{x}_i - \mathbf{x}_j) : \boldsymbol{\varepsilon}^{*0}_{(j)} + \mathbf{s} : \overline{\mathbf{d}}^*_{(i)} + \mathbf{G}^1(\mathbf{x}_i - \mathbf{x}_j) : \overline{\mathbf{d}}^*_{(j)} + O(\rho^8), \tag{20}$$

where

$$\mathbf{G}^1 \equiv \int\limits_{\Omega_1} \mathbf{G}(\mathbf{x} - \mathbf{x}_2)\, \mathbf{dx} = \int\limits_{\Omega_2} \mathbf{G}(\mathbf{x}_1 - \mathbf{x})\, \mathbf{dx} = \frac{1}{30\ (1 - \nu_0)}\ (\rho^3 \mathbf{H}^1 + \rho^5\ \mathbf{H}^2), \tag{21}$$

$$\mathbf{G}^2 \equiv \frac{1}{\Omega} \int\limits_{\Omega_1} \int\limits_{\Omega_2} \mathbf{G}(\mathbf{x} - \mathbf{x}')\, \mathbf{dx}'\, \mathbf{dx} = \frac{1}{30\ (1 - \nu_0)}\ (\rho^3\ \mathbf{H}^1 + 2\rho^5\ \mathbf{H}^2), \tag{22}$$

and the components of $\mathbf{H}^1$ and $\mathbf{H}^2$ are rendered by

$$\mathbf{H}^1_{ijkl}(\mathbf{x}_1 - \mathbf{x}_2) \equiv 5\ \mathbf{F}_{ijkl}(-15, 3\nu_0, 3, 3 - 6\nu_0, -1 + 2\nu_0, 1 - 2\nu_0), \tag{23}$$

$$\mathbf{H}^2_{ijkl}(\mathbf{x}_1 - \mathbf{x}_2) \equiv 3\ \mathbf{F}_{ijkl}(35, -5, -5, -5, 1, 1). \tag{24}$$

It is noted that the leading-order error induced by dropping the higher order moments in Eq. (20) is of the order $O(\rho^8)$ since $\overline{\mathbf{P}}^*_{(i)}$ and $\Omega a \nabla_{\mathbf{x}} \otimes \mathbf{G}$ are of the order $O(\rho^4)$.
Moreover, Eq. (20) can be recast as

$$(\mathbf{A}_1 + \mathbf{s}) : \overline{\mathbf{d}}^*_{(1)} + \mathbf{G}^1 : \overline{\mathbf{d}}^*_{(2)} = -\mathbf{G}^2 : \boldsymbol{\varepsilon}^{*0}_{(2)}, \tag{25}$$

$$\mathbf{G}^1 : \overline{\mathbf{d}}^*_{(1)} + (\mathbf{A}_2 + \mathbf{s}) : \overline{\mathbf{d}}^*_{(2)} = -\mathbf{G}^2 : \boldsymbol{\varepsilon}^{*0}_{(1)}. \tag{26}$$

Therefore, the solutions of Eqs. (25) and (26) are

$$\overline{\mathbf{d}}^*_{(1)} = \left[(\mathbf{G}^1)^{-1} \bullet (\mathbf{A}_1 + \mathbf{s}) - (\mathbf{A}_2 + \mathbf{s})^{-1} \bullet \mathbf{G}^1\right]^{-1} \left[(\mathbf{A}_2 + \mathbf{s})^{-1} \bullet \mathbf{G}^2 : \boldsymbol{\varepsilon}^{*0}_{(1)} - (\mathbf{G}^1)^{-1} \bullet \mathbf{G}^2 : \boldsymbol{\varepsilon}^{*0}_{(2)}\right], \tag{27}$$

$$\overline{\mathbf{d}}^*_{(2)} = \left[(\mathbf{A}_1 + \mathbf{s})^{-1} \bullet \mathbf{G}^1 - (\mathbf{G}^1)^{-1} \bullet (\mathbf{A}_2 + \mathbf{s})\right]^{-1} \left[(\mathbf{G}^1)^{-1} \bullet \mathbf{G}^2 : \boldsymbol{\varepsilon}^{*0}_{(1)} - (\mathbf{A}_1 + \mathbf{s})^{-1} \bullet \mathbf{G}^2 : \boldsymbol{\varepsilon}^{*0}_{(2)}\right], \tag{28}$$

where the leading orders of $(\mathbf{A}_2 + \mathbf{s})^{-1} \bullet \mathbf{G}^1$ and $(\mathbf{G}^1)^{-1} \bullet (\mathbf{A}_1 + \mathbf{s})$ are of the order $O(\rho^3)$ and $O(\rho^{-3})$ in Eq. (27), respectively. It is interesting to note that $(\mathbf{A}_2 + \mathbf{s})^{-1} \bullet \mathbf{G}^1$ is truncated since its leading order is greater than the leading order of $(\mathbf{G}^1)^{-1} \bullet (\mathbf{A}_1 + \mathbf{s})$. We also have $\rho < 1/2$.

Therefore, the solution of Eq. (27) is

$$\overline{\mathbf{d}}^*_{(1)} = (\mathbf{A}_1 + \mathbf{s})^{-1} \bullet (\mathbf{G}^1) \bullet (\mathbf{A}_2 + \mathbf{s})^{-1} \bullet \mathbf{G}^2 : \boldsymbol{\varepsilon}^{*0}_{(1)} - (\mathbf{A}_1 + \mathbf{s})^{-1} \bullet \mathbf{G}^2 : \boldsymbol{\varepsilon}^{*0}_{(2)}. \tag{29}$$

Similarly, Eq. (28) can be rephrased as

$$\overline{\mathbf{d}}^*_{(2)} = (\mathbf{A}_2 + \mathbf{s})^{-1} \bullet (\mathbf{G}^1) \bullet (\mathbf{A}_1 + \mathbf{s})^{-1} \bullet \mathbf{G}^2 : \boldsymbol{\varepsilon}^{*0}_{(2)} - (\mathbf{A}_2 + \mathbf{s})^{-1} \bullet \mathbf{G}^2 : \boldsymbol{\varepsilon}^{*0}_{(1)}. \tag{30}$$

3 Effective elastic moduli of three-phase composites

3.1 Ensemble-volume averaged eigenstrains

To obtain the probabilistic ensemble-averaged solution of $\overline{\mathbf{d}}^{*}_{(i)}$ within the context of approximate pairwise local particle interaction, one has to integrate Eqs. (29) and (30) over all possible positions $(\mathbf{x}_j)$ of the second particle for a given location of the first particle $(\mathbf{x}_i)$. The ensemble-average process takes the form

$$\left\langle \overline{\mathbf{d}}^{*}_{(i)} \right\rangle (\mathbf{x}_i) = \int\limits_{V-\Omega_i} \overline{\mathbf{d}}^{*}_{(i)}(\mathbf{x}_i - \mathbf{x}_j)\; P(\mathbf{x}_j \,|\mathbf{x}_i)\; \mathbf{d}\mathbf{x}_j \;, \quad i \neq j, \tag{31}$$

in which $P(\mathbf{x}_j \,|\mathbf{x}_i)$ is the conditional probability density function for finding the second particle centered at $\mathbf{x}_j$ given the first particle centered at $\mathbf{x}_i$. Moreover, angled brackets define the ensemble-average operator. In this paper, a three-dimensional statistically isotropic and homogeneous two-point probability density function $P(\mathbf{x}_j \,|\mathbf{x}_i)$ is considered. The three-dimensional isotropic probabilistic integration domain V in Eq. (31) can therefore be evaluated as a sphere. Further, Ω_i in Eq. (31) defines the probabilistic "exclusion zone" for $\mathbf{x}_j$.

The two-point conditional probability function $P(\mathbf{x}_j \,|\mathbf{x}_i)$ is determined by the microstructure of a composite, which in turn depends on the particle volume fraction and underlying manufacturing processes. For illustration, the two-point conditional probability density function is taken as statistically isotropic and uniform, and obeys the following:

$$P(\mathbf{x}_j \,|\mathbf{x}_i) \;= \begin{cases} \frac{N}{V} & \text{if } r \geq 2a, \\ 0 & \text{otherwise}, \end{cases} \tag{32}$$

where $\frac{N}{V}$ is the three-dimensional number density of particles in a composite and r is the spacing between the centers of two spheres. By substituting Eq. (29) into (31), the explicit expression for $\left\langle \overline{\mathbf{d}}^{*}_{(1)} \right\rangle (\mathbf{x}_1)$ can be depicted as

$$\begin{aligned} \left\langle \overline{\mathbf{d}}^{*}_{(1)} \right\rangle (\mathbf{x}_1) = & \left[\int\limits_{2a}^{\infty} \int\limits_{\Xi} P(\mathbf{x}_2 \,|\mathbf{x}_1)\; (\mathbf{A}_1 + \mathbf{s})^{-1} \bullet (\mathbf{G}^1) \bullet (\mathbf{A}_2 + \mathbf{s})^{-1} \bullet \mathbf{G}^2 \; \mathrm{d}\Xi \;\; \mathrm{d}r \right] : \boldsymbol{\varepsilon}^{*0}_{(1)} \\ & - \left[\int\limits_{2a}^{\infty} \int\limits_{\Xi} P(\mathbf{x}_2 \,|\mathbf{x}_1)\; (\mathbf{A}_1 + \mathbf{s})^{-1} \bullet \mathbf{G}^2 \; \mathrm{d}\Xi \;\; \mathrm{d}r \right] : \boldsymbol{\varepsilon}^{*0}_{(2)}, \end{aligned} \tag{33}$$

where Ξ signifies the spherical surface of radius r.

In what follows, we present two non-equivalent formulations to predict the effective elastic moduli of three-phase composites, involving "Formulation I" here and "Formulation II" in Sect. 3.2. Specifically, the following identities can be easily proved:

$$\int\limits_{\Xi} n_i \; n_j \; \mathrm{d}\Xi = \frac{4\pi r^2}{3} \delta_{ij}, \tag{34}$$

$$\int\limits_{\Xi} n_i \; n_j \; n_k \; n_l \; \mathrm{d}\Xi = \frac{4\pi r^2}{15} \; (\delta_{ij} \; \delta_{kl} + \delta_{ik} \; \delta_{jl} + \delta_{il} \; \delta_{jk}), \tag{35}$$

where $\mathbf{n}$ is the normal vector at a point on Ξ; i.e., $\mathbf{n} = \mathbf{r}/r$ with $\mathbf{r} = \mathbf{x}_2 - \mathbf{x}_1$. Using Eqs. (21)–(22) and Eqs. (34)–(35), it is straightforward to verify that the surface integral of $(\mathbf{A}_1 + \mathbf{s})^{-1} \bullet \mathbf{G}^2$ in the second line of Eq. (33) is identically zero. By carrying out the lengthy algebra and utilizing the identities (34)–(35), the ensemble integration for $\left\langle \overline{\mathbf{d}}^{*}_{(1)} \right\rangle (\mathbf{x}_1)$ reads

$$\begin{aligned} \left\langle \overline{\mathbf{d}}^{*}_{(1)} \right\rangle (\mathbf{x}_1) = & \left\{ \phi_2 \left(q_1 + \frac{90}{64\beta_1\beta_2} \right) \delta_{ij}\delta_{kl} + \phi_2 \left(q_2 - \frac{135}{64\beta_1\beta_2} \right) (\delta_{ik}\delta_{jl} + \delta_{il}\delta_{jk}) \right. \\ & \left. + \; \phi_1 \left(q_3 + \frac{90}{64\beta_1^2} \right) \delta_{ij}\delta_{kl} + \phi_1 \left(q_4 - \frac{135}{64\beta_1^2} \right) (\delta_{ik}\delta_{jl} + \delta_{il}\delta_{jk}) \right\} : \boldsymbol{\varepsilon}^{*0}_{(1)}. \end{aligned} \tag{36}$$

Here, $\phi_i = \frac{N_i}{V}\left(\frac{4}{3}\pi a^3\right)$, with $i = 1, 2$, is the volume fraction of the i-phase particle. Other parameters in the above equation are summarized in Appendix A.

The approximate ensemble-volume averaged eigenstrain tensor can be derived from Eqs. (17) and (32), and takes the form

$$\left\langle \overline{\boldsymbol{\varepsilon}}^*_{(1)} \right\rangle = \boldsymbol{\Gamma}^1 : \boldsymbol{\varepsilon}^{*0}_{(1)}. \tag{37}$$

Here, the components of the isotropic tensor $\boldsymbol{\Gamma}^1$ are

$$\boldsymbol{\Gamma}^1_{ijkl} = r_1\ \delta_{ij}\delta_{kl} + r_2\ (\delta_{ik}\delta_{jl} + \delta_{il}\delta_{jk}) \tag{38}$$

in which

$$r_1 = \phi_2\ t_1 + \phi_1\ t_3, \quad r_2 = \frac{1}{2} + \phi_2\ t_2 + \phi_1\ t_4 \tag{39}$$

with

$$t_1 = q_1 + \frac{90}{64}\left(\frac{1}{\beta_1\beta_2}\right), \quad t_2 = q_2 - \frac{135}{64}\left(\frac{1}{\beta_1\beta_2}\right), \quad t_3 = q_3 + \frac{90}{64}\left(\frac{1}{\beta_1^2}\right), \quad t_4 = q_4 - \frac{135}{64}\left(\frac{1}{\beta_1^2}\right). \tag{40}$$

Similarly, the approximate ensemble-volume averaged eigenstrain tensor $\left\langle \overline{\boldsymbol{\varepsilon}}^*_{(2)} \right\rangle$ reads

$$\left\langle \overline{\boldsymbol{\varepsilon}}^*_{(2)} \right\rangle = \boldsymbol{\Gamma}^2 : \boldsymbol{\varepsilon}^{*0}_{(2)}. \tag{41}$$

The components of the isotropic tensor $\boldsymbol{\Gamma}^2$ are

$$\boldsymbol{\Gamma}^2_{ijkl} = r_3\ \delta_{ij}\delta_{kl} + r_4\ (\delta_{ik}\delta_{jl} + \delta_{il}\delta_{jk}), \tag{42}$$

where

$$r_3 = \phi_1\ t_5 + \phi_2\ t_7, \quad r_4 = \frac{1}{2} + \phi_1\ t_6 + \phi_2\ t_8. \tag{43}$$

Other parameters in Eqs. (42) and (43) are exhibited in Appendix B.

3.2 Effective bulk and shear moduli of three-phase composites containing randomly dispersed spherical particles

In this section, we derive effective elastic moduli of composites containing many randomly dispersed spherical particles of different elastic properties. We shall utilize the probabilistic ensemble-volume averaged pairwise local interaction solutions for $\left\langle \overline{\varepsilon}^*_{(i)} \right\rangle$ and other ensemble-volume averaged field equations. In what follows, angle brackets for the ensemble-average operators will be dropped for compactness.

According to Ju and Chen [13] and Zhao et al. [37], the following relations governing the ensemble-volume averaged stress $\overline{\boldsymbol{\sigma}}$, the averaged strain $\overline{\boldsymbol{\varepsilon}}$, the uniform remote strain $\boldsymbol{\varepsilon}^0$ and the averaged eigenstrain $\overline{\boldsymbol{\varepsilon}}^*_{(i)}$ take the form

$$\overline{\boldsymbol{\sigma}} = \mathbf{C}_0 : \left(\overline{\boldsymbol{\varepsilon}} - \sum_{i=1}^{2} \phi_i\ \overline{\boldsymbol{\varepsilon}}^*_{(i)}\right), \tag{44}$$

$$\overline{\boldsymbol{\varepsilon}} = \boldsymbol{\varepsilon}^0 + \sum_{i=1}^{2} \phi_i\ \mathbf{s} : \overline{\boldsymbol{\varepsilon}}^*_i. \tag{45}$$

Upon substitution of the solution of $\overline{\boldsymbol{\varepsilon}}^*_{(i)}$ in Eqs. (37) and (41) into Eq. (45), and invoking the relation between $\boldsymbol{\varepsilon}^0$ and $\boldsymbol{\varepsilon}^{*0}_{(i)}$ given by Eq. (9), the relations between the averaged eigenstrain $\overline{\boldsymbol{\varepsilon}}^*_{(i)}$ and the averaged strain $\overline{\boldsymbol{\varepsilon}}$ are rendered as

$$\overline{\boldsymbol{\varepsilon}}^*_{(1)} = \boldsymbol{\Gamma}^1 \bullet \left(\mathbf{T}^1\right)^{-1} : \overline{\boldsymbol{\varepsilon}}, \quad \overline{\boldsymbol{\varepsilon}}^*_{(2)} = \boldsymbol{\Gamma}^2 \bullet \left(\mathbf{T}^2\right)^{-1} : \overline{\boldsymbol{\varepsilon}}, \tag{46}$$

where

$$\mathbf{T}^1 = \left(-\mathbf{A}_1 - \mathbf{s} + \phi_1\ \mathbf{s}\bullet\mathbf{\Gamma}^1 + \phi_2\ \mathbf{s}\bullet\mathbf{\Gamma}^2\bullet(\mathbf{A}_2+\mathbf{s})^{-1}\bullet(\mathbf{A}_1+\mathbf{s})\right), \tag{47}$$

$$\mathbf{T}^2 = \left(-\mathbf{A}_2 - \mathbf{s} + \phi_2\ \mathbf{s}\bullet\mathbf{\Gamma}^2 + \phi_1\ \mathbf{s}\bullet\mathbf{\Gamma}^1\bullet(\mathbf{A}_1+\mathbf{s})^{-1}\bullet(\mathbf{A}_2+\mathbf{s})\right). \tag{48}$$

Substituting Eq. (46) into (44) leads to the effective stiffness $\mathbf{C}_*$ relating $\overline{\boldsymbol{\sigma}}$ and $\overline{\boldsymbol{\varepsilon}}$:

$$\mathbf{C}_* = \mathbf{C}_0\bullet\left\{\ \mathbf{I} - \phi_1\mathbf{\Gamma}^1\bullet(\mathbf{T}^1)^{-1} - \phi_2\ \mathbf{\Gamma}^2\bullet(\mathbf{T}^2)^{-1}\ \right\}. \tag{49}$$

Since all fourth-rank tensors on the right-hand side of Eq. (49) are isotropic in three dimensions, the effective stiffness tensor $\mathbf{C}_*$ for a three-phase composite is isotropic as well. Further, the effective bulk modulus κ_* and shear modulus μ_* can be explicitly derived as

$$\kappa_* = \kappa_0\left(1 + \frac{30(1-\nu_0)\ [\omega_2\ \phi_1(3r_1+2r_2) + \omega_1\ \phi_2(3r_3+2r_4)]}{\omega_1\ \omega_2 - 10(1+\nu_0)\ [\omega_2\ \phi_1(3r_1+2r_2) + \omega_1\ \phi_2(3r_3+2r_4)]}\right), \tag{50}$$

$$\mu_* = \mu_0\left(1 + \frac{30\ (1-\nu_0)\ (\beta_2\phi_1 r_2 + \beta_1\phi_2 r_4)}{\beta_1\beta_2 - 4(4-5\nu_0)\ (\beta_2\phi_1 r_2 + \beta_1\phi_2 r_4)}\right), \tag{51}$$

where $\omega_i = 3\alpha_i + 2\beta_i$ and $i = 1, 2$. In addition, r_1, r_2, r_3 and r_4 have previously been defined by Eqs. (39) and (43).

We now consider an interesting special case involving the non-equivalent "Formulation II" by neglecting the higher-order components $O(\rho^5)$ in Eqs. (21) and (22). Following a similar procedure as in "Formulation I" in Sect. 3.1, the approximate ensemble-volume averaged eigenstrain tensors become

$$\left\langle\overline{\boldsymbol{\varepsilon}}^*_{(1)}\right\rangle = \mathbf{\Gamma}^1 : \boldsymbol{\varepsilon}^{*0}_{(1)} \quad \text{and} \quad \left\langle\overline{\boldsymbol{\varepsilon}}^*_{(2)}\right\rangle = \mathbf{\Gamma}^2 : \boldsymbol{\varepsilon}^{*0}_{(2)}, \tag{52}$$

where the components of the isotropic tensors $\mathbf{\Gamma}^1$ and $\mathbf{\Gamma}^2$ read

$$\mathbf{\Gamma}^1_{ijkl} = r_1\delta_{ij}\delta_{kl} + r_2(\delta_{ik}\delta_{jl} + \delta_{il}\delta_{jk}) \quad \text{and} \quad \mathbf{\Gamma}^2_{ijkl} = r_3\delta_{ij}\delta_{kl} + r_4(\delta_{ik}\delta_{jl} + \delta_{il}\delta_{jk}). \tag{53}$$

with

$$r_1 = \phi_2 q_1 + \phi_1 q_3, \quad r_2 = \frac{1}{2} + \phi_2 q_2 + \phi_1 q_4, \quad r_3 = \phi_1 q_5 + \phi_2 q_7, \quad r_4 = \frac{1}{2} + \phi_1 q_6 + \phi_2 q_8. \tag{54}$$

Other parameters in Eq. (54) are exhibited in Appendices A and B.

The effective bulk modulus κ_* and shear modulus μ_* can be explicitly expressed as

$$\kappa_* = \kappa_0\left(1 + \frac{30(1-\nu_0)\ [\omega_2\phi_1(3r_1+2r_2) + \omega_1\phi_2(3r_3+2r_4)]}{\omega_1\omega_2 - 10(1+\nu_0)\ [\omega_2\phi_1(3r_1+2r_2) + \omega_1\phi_2(3r_3+2r_4)]}\right), \tag{55}$$

$$\mu_* = \mu_0\left(1 + \frac{30(1-\nu_0)\ (\beta_2\phi_1 r_2 + \beta_1\phi_2 r_4)}{\beta_1\beta_2 - 4(4-5\nu_0)(\beta_2\phi_1 r_2 + \beta_1\phi_2 r_4)}\right), \tag{56}$$

where $\omega_i = 3\alpha_i + 2\beta_i$ and $i = 1, 2$. Further, r_1, r_2, r_3 and r_4 are defined by Eq. (54).

In the special event that a matrix material contains identical spherical particles (i.e., $\kappa_1 = \kappa_2, \mu_1 = \mu_2, a_1 = a_2$), Eqs. (55) and (56) reduce to

$$\kappa_* = \kappa_0\left(1 + \frac{30\ (1-\nu_0)\phi(3r_1+2r_2)}{3\alpha + 2\beta - 10(1+\nu_0)\phi(3r_1+2r_2)}\right), \tag{57}$$

$$\mu_* = \mu_0\left(1 + \frac{30(1-\nu_0)\phi r_2}{\beta - 4(4-5\nu_0)\phi r_2}\right), \tag{58}$$

with $\alpha = \alpha_1 = \alpha_2, \quad \beta = \beta_1 = \beta_2, \quad r_1 = r_3, \quad r_2 = r_4$ and $\phi = \phi_1 + \phi_2$. Here, ϕ denotes the total particle volume fraction. It is noted that Eqs. (57)–(58) are entirely identical to Eqs. (23)–(24) in Ju and Tseng [17].

4 Some analytical examples

A number of analytical examples are presented in this section for two-phase and three-phase elastic composites containing many randomly dispersed spherical particles.

4.1 Two-phase elastic composites

For an incompressible matrix containing randomly located and identical rigid spheres, the proposed pairwisely local interacting solution from Eq. (51) reduces to the following effective shear modulus:

$$\mu_* = \mu_0 \left(1 + \frac{5\phi}{2} \frac{32 + 15\phi}{32 - 32\phi - 15\phi^2}\right). \tag{59}$$

Equation (59) becomes singular at $\phi = 0.742$. Nevertheless, the singularity point is irrelevant since the maximum random packing density of identical spherical particles is 0.74. In comparison with Eq. (56) of Ju and Chen [14], it is observed that significant improvement in the singular problem has been achieved by employing the current methodology. Moreover, the Taylor's series expansion of Eq. (59) with respect to ϕ results in

$$\mu_* = \mu_0 \left(1 + \frac{5}{2}\phi + \frac{235}{64}\phi^2 + O(\phi^3)\right). \tag{60}$$

We note that Eqs. (49)–(51) and (59) for effective elastic moduli form an approximate, analytical, higher-order overall micromechanical formulation in ϕ; the proposed framework differs from the second-order overall model in the literature. Comparisons of the second-order truncated solution of Eq. (60) with other existing second-order models are discussed next. The coefficient of $O(\phi^2)$ in Eq. (60) (the shear modulus) is 235/64 (or 3.671875). Our truncated second-order calculation has a considerable difference with other existing second-order calculations. For example, the prediction made by Ju and Chen [14] and Willis and Acton [38] is 4.84375, which is less accurate (in term of ρ) than our truncated second-order result, since an added number of terms in the series solution are required in our current approach. The other calculations of the second-order coefficient of $O(\phi^2)$ made by Batchelor and Green [9], Kim and Mifflin [39] and Chen and Acrivos [12] are 5.2 ± 0.3, 5.07 and 5.01, respectively.

We now take upon the special case of an incompressible matrix containing randomly dispersed identical spherical *microvoids*. According to Eqs. (50)–(51), the corresponding effective bulk and shear moduli of the proposed interacting solutions become

$$\kappa_* = \frac{4}{3}\,\mu_0 \left(\frac{1}{\phi} - 1\right) \quad \text{and} \quad \mu_* = \mu_0 \left(1 - \frac{120\phi + 25\phi^2}{72 + 48\phi + 10\phi^2}\right). \tag{61}$$

It is of some interest to compare the effective bulk and shear moduli in Eq. (61) with Eqs. (46) and (47) made by Ju and Chen [13]. It is observed that the expression for the effective bulk modulus rendered in Eq. (61) is surprisingly the same as the first-order ("non-interacting") result discussed in Eq. (46) by Ju and Chen [13]. On the other hand, Taylor's series expansion of the effective shear modulus in Eq. (61) with respect to ϕ yields

$$\mu_* = \mu_0 \left(1 - \frac{5}{3}\phi + \frac{55}{72}\,\phi^2 + O(\phi^3)\right). \tag{62}$$

The second-order term $\frac{55}{72}\phi^2$ here is very different from that $\left(\frac{10}{9}\phi^2\right)$ of Eq. (47) in Ju and Chen [13] which was derived based on the first-order (non-interacting) formulation.

4.2 Three-phase elastic composites

If the first and the second phases contain identical rigid spheres and identical spherical microvoids, respectively, then we write $\mathbf{A}_1 = \mathbf{0}$ and $\mathbf{A}_2 = -\mathbf{I}$ as a special case. Consequently, the effective bulk (Eq. 50) and shear

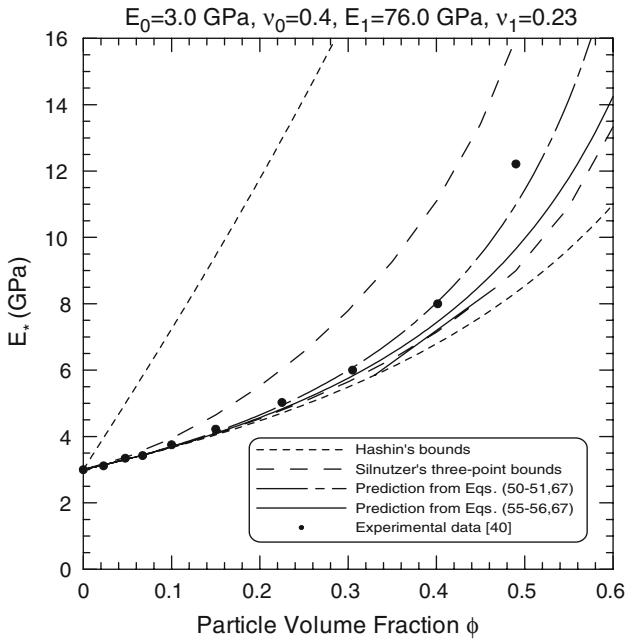

Fig. 2 Effective Young's moduli E_* versus particle volume fractions ϕ, with *solid circles* signifying experimental data from Smith [40]

moduli (Eq. 51) are

$$\kappa_* = \kappa_0 \left(1 + \frac{3(1-\nu_0)}{(1+\nu_0)} \cdot \frac{2(1-2\nu_0)\phi_1(3r_1+2r_2) - (1+\nu_0)\phi_2(3r_3+2r_4)}{2(1-2\nu_0)\left[1-\phi_1(3r_1+2r_2)\right] + (1+\nu_0)\phi_2(3r_3+2r_4)}\right), \tag{63}$$

$$\mu_* = \mu_0 \left(1 + \frac{30(1-\nu_0)}{(8-10\nu_0)} \cdot \frac{(7-5\nu_0)\phi_1 r_2 - (8-10\nu_0)\phi_2 r_4}{(7-5\nu_0)(1-2\phi_1 r_2) + 2(8-10\nu_0)\phi_2 r_4}\right). \tag{64}$$

In addition, if one entirely neglects the local particle interaction effects, then $\mathbf{\Gamma}^1$ in Eq. (37) and $\mathbf{\Gamma}^2$ in Eq. (41) would reduce to $\mathbf{I}$ at the same time. Accordingly, the effective bulk κ_* and shear modulus μ_* become:

$$\kappa_* = \kappa_0 \left(1 + \frac{3(1-\nu_0)}{(1+\nu_0)} \cdot \frac{2(1-2\nu_0)\phi_1 - (1+\nu_0)\phi_2}{2(1-2\nu_0)(1-\phi_1) + (1+\nu_0)\phi_2}\right), \tag{65}$$

$$\mu_* = \mu_0 \left(1 + \frac{15(1-\nu_0)}{(8-10\nu_0)} \cdot \frac{(7-5\nu_0)\phi_1 - (8-10\nu_0)\phi_2}{(7-5\nu_0)(1-\phi_1) + (8-10\nu_0)\phi_2}\right). \tag{66}$$

It is observed that these first-order ("non-interacting") expressions are identical to Eqs. (48) and (49) in Ju and Chen [13], as expected.

To further assess the capability of the proposed micromechanical framework, the analytical predictions with particle interaction effects are compared with the two-point bounds (Hashin and Shtrikman [3]), the three-point bounds (Milton and Phan-Thien [11], Torquato and Lado [4]), and experimental data (Smith [40], Walsh et al. [41]). The following material properties of two separate experiments are taken as follows: (i) $E_0 = 3.0$GPa, $\nu_0 = 0.4$, $E_1 = 76.0$GPa and $\nu_1 = 0.23$ from Smith's [40] data; (ii) $E_0 = 0.75 \times 10^6$bars and $\nu_0 = 0.23$ with spherical voids of volume fractions ranging from 0 to 0.5, based on Walsh et al. [41]. Figure 2 displays the predicted effective Young's moduli at various particle volume fractions ϕ. Here, the effective Young's modulus E_* can be easily obtained through the expression

$$E_* = \frac{9\kappa_*\mu_*}{3\kappa_* + \mu_*}. \tag{67}$$

We exhibit the theoretical predictions in Fig. 2 based on Hashin's second-order bounds [3], the third-order bounds [4,6], the proposed "Formulation I" Eqs. (50)–(51) and (67), as well as the simplified "Formulation

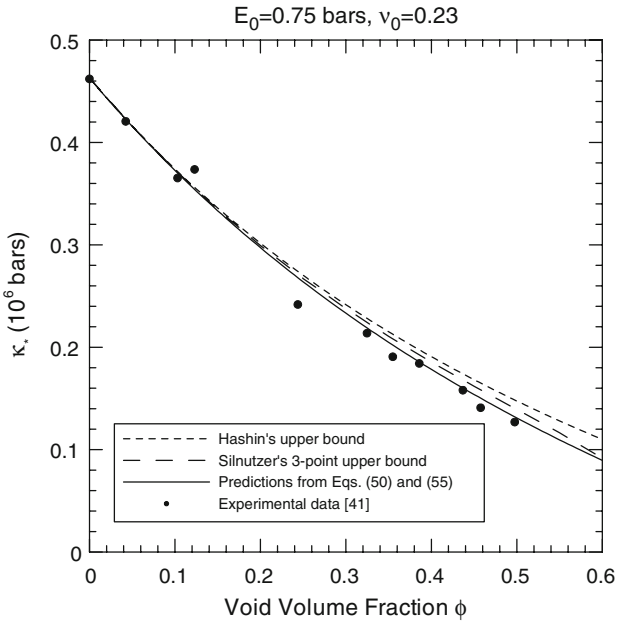

Fig. 3 Effective bulk moduli versus void volume fractions ϕ, with *solid circles* signifying experimental data from [41]

II" Eqs. (55)–(56) and (67), respectively. In addition, the experimental data of [40] are rendered in Fig. 2 for comparison purposes. As a special case, the proposed formulations rendered in Eqs. (50)–(51) and (55)–(56) reduce to the two-phase formulas as expected; i.e., phase 1 is entirely identical to phase 2. Clearly, our analytical predictions are well within Hashin's second-order bounds [3] and the third-order bounds [4,6].

Figure 3 exhibits comparisons among our analytical predictions (Eqs. (50) and (55)), Hashin's second-order upper bound [3], the third-order upper bound [4,6], and Walsh et al. experimental data [41] on effective bulk moduli κ_* of porous glasses. We observe that the closed-form predictions of Eqs. (50) and (55) are identical in this special case. It is also interesting to note that the proposed formulation compares very well with experimental data for void volume fractions ϕ up to about 50%. Based on the foregoing preliminary analytical and experimental comparisons, the proposed micromechanical approach offers a simple, approximate, yet sufficiently accurate framework for the predictions of effective elastic moduli of two-phase composites containing randomly dispersed elastic spherical particles.

Next, we proceed to assess the validity of the proposed micromechanical framework in predicting effective elastic properties of three-phase composites (e.g., an elastic matrix with randomly dispersed spherical particles and voids). Experimental studies to characterize three-phase evolutions and statistical microstructures in composites are still much needed in the literature. In the absence of actual manufacturing and microstructural evidences, it is assumed that micro-defects such as voids exist often in composite materials. For convenience, we adopt the same material parameters of Smith's experiment [40] as discussed earlier. The predictions of effective Young's moduli at various void volume fractions (phase 2) with different particle volume fractions (phase 1) are shown in Fig. 4, where ϕ_1 and ϕ_2 define the volume fractions of particles and voids, respectively. Unless noted otherwise, in subsequent analytical simulations the matrix properties are taken as Young's modulus $E_0 = 3.0$GPa and Poisson's ratio $\nu_0 = 0.4$.

To examine the effects of varying Young's moduli (E_2) of the second-phase particles, we perform various micromechanics-based predictions in Figs. 5 and 6. Specifically, Figs. 5 and 6 show the predicted effective (normalized) bulk moduli κ_*/κ_0 and effective (normalized) shear moduli μ_*/μ_0 of three-phase composites at various particle volume fractions ϕ_2 (phase 2) with a constant particle volume fraction ϕ_1 (phase 1). Here, we employ the particle parameters as follows: $E_1/E_0 = 20$, $\nu_1 = 0.2$, $\phi_1 = 0.1$, and $\nu_2 = 0.2$. Various E_2/E_0 ratios are displayed in Figs. 5 and 6. From these results, it is clear that higher Young's modulus ratio E_2/E_0 leads to higher effective (normalized) bulk modulus κ_*/κ_0 and higher effective (normalized) shear modulus μ_*/μ_0.

Further, we consider three-phase composites consisting of an elastic matrix, spherical rigid particles (phase 1), and spherical voids (phase 2). The analytical predictions of effective (normalized) bulk moduli

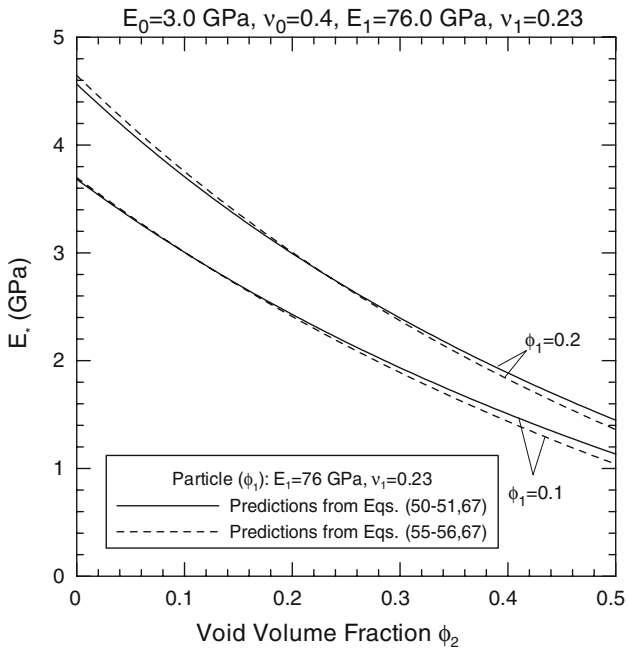

Fig. 4 Effective Young's moduli versus void volume fractions ϕ_2, with different particle volume fractions ($\phi_1 = 0.1, 0.2$)

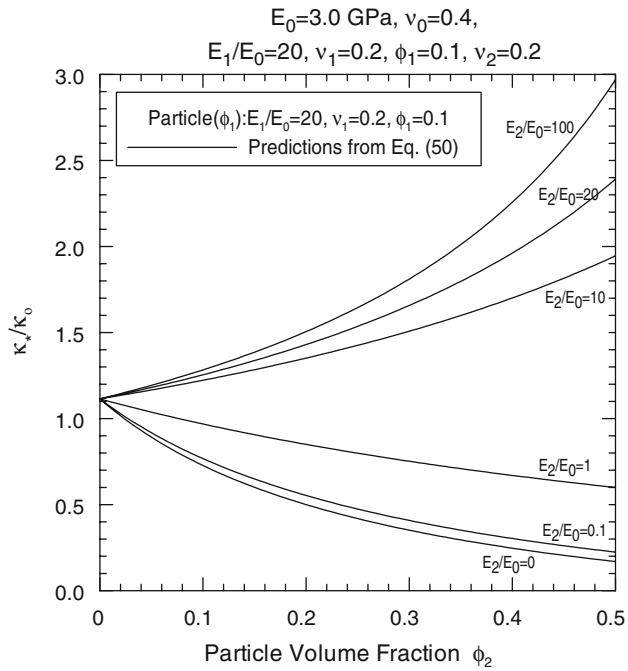

Fig. 5 The predicted effective (normalized) bulk moduli κ_*/κ_0 of three-phase composites versus particle volume fractions ϕ_2 (phase 2) with constant particle volume fraction ϕ_1 (phase 1)

κ_*/κ_0 from the proposed micromechanical higher-order interaction formulation (Eq. 63) and the first-order "non-interacting" formulation (Eq. 65) are compared in Fig. 7. No available experimental data are found at this time for comparison. The differences in effective (normalized) bulk moduli κ_*/κ_0 between the proposed higher-order and the first-order formulations increase as rigid volume fractions (ϕ_1) increase in Fig. 7.

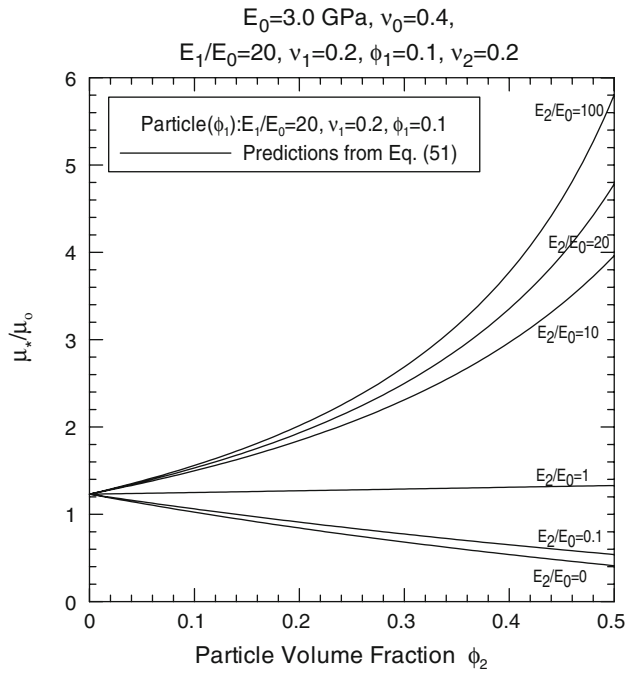

Fig. 6 The predicted effective (normalized) shear moduli μ_*/μ_0 of three-phase composites versus particle volume fractions ϕ_2 (phase 2) with constant particle volume fraction ϕ_1 (phase 1)

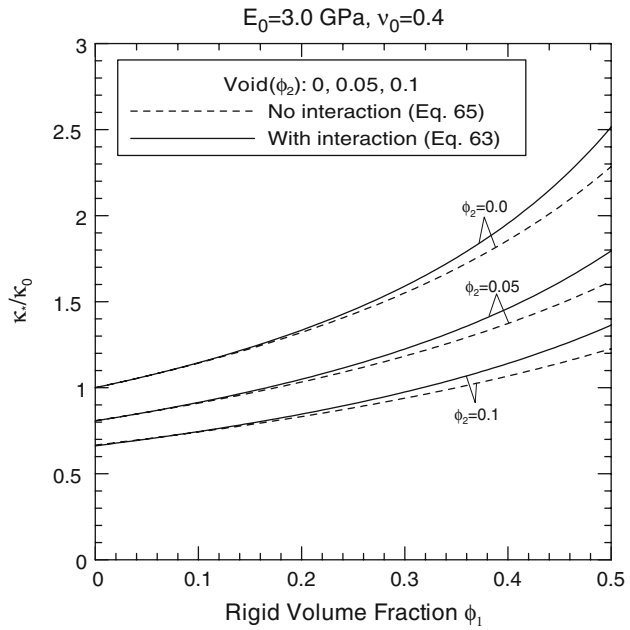

Fig. 7 The predicted effective (normalized) bulk moduli κ_*/κ_0 of three-phase composites versus rigid particle volume fractions (ϕ_1) with different void volume fractions ($\phi_2 = 0, 0.05, 0.1$)

5 Conclusions

Based on the governing micromechanical field equations and the approximate (higher-order) pairwise particle interaction solutions, new micromechanical formulations have been presented in this work to predict effective elastic moduli of three-phase composites containing randomly dispersed spherical particles of distinct elastic properties. The effects of random dispersion of spherical particles are accounted for through the probabilistic

ensemble averaging process. The ensemble-volume averaged eigenstrains in particles are approximately yet accurately evaluated by Eqs. (37) and (41) through the pairwise particle interactions. Hence, a compact analytical formula (49) is derived. As a result, two different analytical formulas of effective elastic moduli have been derived in Sect. 3. The present paper represents a significant improvement over the previous work of Ju and Chen [14] (and other researchers) which is based on the identical spherical particles on the matrix. Moreover, the present higher-order prediction (in ρ) in Eq. (36) is compared with that of Ju and Chen [14]. The two formulations, corresponding to Eqs. (50)–(51) and (55)–(56), both reduce to the formulas of two-phase elastic composites, and are compared with Hashin's second-order bounds [3], the third-order bounds [4,6], and select experimental data. These comparisons and simulations encompass particle reinforced elastic composites, elastic matrices with randomly dispersed particles and voids, and rigid particles and voids. No Monte Carlo simulations or finite element calculations are needed here.

The authors are currently working on the extension of the proposed methodology to predict effective elastic moduli of multi-phase composites containing randomly dispersed spherical particles of distinct properties and different sizes. The methods proposed by Ju and Chen [14] and the present authors will be adopted to construct micromechanical ensemble-volume averaged estimates of the aforementioned analytical extension.

Acknowledgments This work was in part sponsored by the Faculty Research Grant of the Academic Senate of UCLA (Fund Number 4-592565-19914) and in part by Bellagio Engineering.

Appendix A

The parameters in Eq. (36) take the form:

$$q_1 = \frac{-5}{4}\left\{\frac{\alpha_1\left[2\beta_2\left(11-11\nu_0+5\nu_0^2\right)+3\alpha_2\left(10-10\nu_0+7\nu_0^2\right)\right]}{\beta_1\beta_2\left(3\alpha_1+2\beta_1\right)\left(3\alpha_2+2\beta_2\right)} + \frac{2\beta_1\left[2\beta_2\left(2-2\nu_0+5\nu_0^2\right)+\alpha_2\left(5-5\nu_0+17\nu_0^2\right)\right]}{\beta_1\beta_2\left(3\alpha_1+2\beta_1\right)\left(3\alpha_2+2\beta_2\right)}\right\}, \tag{68}$$

$$q_2 = \frac{5}{8}\left\{\frac{2\beta_2\left(11-11\nu_0+5\nu_0^2\right)+3\alpha_2\left(10-10\nu_0+7\nu_0^2\right)}{\beta_1\beta_2\left(3\alpha_2+2\beta_2\right)}\right\}, \tag{69}$$

$$q_3 = \frac{-5}{4}\left\{\frac{2\beta_1\left(2-2\nu_0+5\nu_0^2\right)+\alpha_1\left(10-10\nu_0+7\nu_0^2\right)}{\beta_1^2\left(3\alpha_1+2\beta_1\right)}\right\}, \tag{70}$$

$$q_4 = \frac{5}{8}\left\{\frac{2\beta_1\left(11-11\nu_0+5\nu_0^2\right)+3\alpha_1\left(10-10\nu_0+7\nu_0^2\right)}{\beta_1^2\left(3\alpha_1+2\beta_1\right)}\right\}, \tag{71}$$

with

$$\alpha_m = 2\left(5\nu_0-1\right)+10\left(1-\nu_0\right)\left(\frac{\kappa_0}{\kappa_m-\kappa_0}-\frac{\mu_0}{\mu_m-\mu_0}\right), \tag{72}$$

$$\beta_m = 2\left(4-5\nu_0\right)+15\left(1-\nu_0\right)\left(\frac{\mu_0}{\mu_m-\mu_0}\right), \quad m=1,2, \tag{73}$$

where κ_0, κ_m and μ_0, μ_m denote the bulk and shear moduli of the matrix and the m-phase particle.

Appendix B

The parameters in Eqs. (42)–(43) are derived as follows:

$$t_5 = q_5+\frac{90}{64}\left(\frac{1}{\beta_1\beta_2}\right);\quad t_6 = q_6-\frac{135}{64}\left(\frac{1}{\beta_1\beta_2}\right);\quad t_7 = q_7+\frac{90}{64}\left(\frac{1}{\beta_2^2}\right);\quad t_8 = q_8-\frac{135}{64}\left(\frac{1}{\beta_2^2}\right); \tag{74}$$

$$q_5 = \frac{-5}{4}\left\{\frac{\alpha_2\left[2\beta_1\left(11-11\nu_0+5\nu_0^2\right)+3\alpha_1\left(10-10\nu_0+7\nu_0^2\right)\right]}{\beta_1\beta_2\left(3\alpha_1+2\beta_1\right)\left(3\alpha_2+2\beta_2\right)}\right.$$
$$\left.+\frac{2\beta_2\left[2\beta_1\left(2-2\nu_0+5\nu_0^2\right)+\alpha_1\left(5-5\nu_0+17\nu_0^2\right)\right]}{\beta_1\beta_2\left(3\alpha_1+2\beta_1\right)\left(3\alpha_2+2\beta_2\right)}\right\}, \tag{75}$$

$$q_6 = \frac{5}{8}\left\{\frac{2\beta_1\left(11-11\nu_0+5\nu_0^2\right)+3\alpha_1\left(10-10\nu_0+7\nu_0^2\right)}{\beta_1\beta_2\left(3\alpha_1+2\beta_1\right)}\right\}, \tag{76}$$

$$q_7 = \frac{-5}{4}\left\{\frac{2\beta_2\left(2-2\nu_0+5\nu_0^2\right)+\alpha_2\left(10-10\nu_0+7\nu_0^2\right)}{\beta_2^2\left(3\alpha_2+2\beta_2\right)}\right\}, \tag{77}$$

$$q_8 = \frac{5}{8}\left\{\frac{2\beta_2\left(11-11\nu_0+5\nu_0^2\right)+3\alpha_2\left(10-10\nu_0+7\nu_0^2\right)}{\beta_2^2\left(3\alpha_2+2\beta_2\right)}\right\}. \tag{78}$$

References

1. Hashin, Z., Shtrikman, S.: On some variational principles in anisotropic and nonhomogeneous elasticity. J. Mech. Phys. Solids **10**, 335–342 (1962)
2. Hashin, Z., Shtrikman, S.: A variational approach to the theory of the elastic behavior of polycrystals. J. Mech. Phys. Solids **10**, 343–352 (1962)
3. Hashin, Z., Shtrikman, S.: A variational approach to the theory of the elastic behavior of multiphase materials. J. Mech. Phys. Solids **11**, 127–140 (1963)
4. Torquato, S., Lado, F.: Effective properties of two-phase disordered composite media: II. Evaluation of bounds on the conductivity and bulk modulus of dispersions of impenetrable spheres. Phys. Rev. **B 33**, 6428–6434 (1986)
5. Mori, T., Tanaka, K.: Average stress in matrix and average elastic energy of materials with misfitting inclusions. Acta Metall. **21**, 571–574 (1973)
6. Sen, A.K., Lado, F., Torquato, S.: Bulk properties of composite media: II. Evaluation of bounds on the shear moduli of suspensions of impenetrable spheres. J. Appl. Phys. **62**, 4135–4141 (1987)
7. Nemat-Nasser, S., Hori, M.: Micromechanics: overall properties of heterogeneous materials, 2nd edn. North-Holland, Amsterdam (1999)
8. Eshelby, J.D.: The determination of the elastic field of an ellipsoidal inclusion, and related problem. Proc. R. Soc. **A241**, 376–396 (1957)
9. Batchelor, G.K., Green, J.T.: The determination of the bulk stress in a suspension of spherical particles to order c^2. J. Fluid Mech. **56**, 401–427 (1972)
10. Silnutzer, N.: Effective Constants of Statistically Homogeneous Materials. Ph.D. Thesis, University of Pennsylvania (1972)
11. Milton, G.W., Phan-Thien, N.: New bounds on effective elastic moduli of two-component materials. Proc. R. Soc. **A380**, 305–331 (1982)
12. Chen, H.S., Acrivos, A.: The effective elastic moduli of composite materials containing spherical inclusions at non-dilute concentrations. Int. J. Solids Struct. **14**, 349–364 (1978)
13. Ju, J.W., Chen, T.M.: Micromechanics and effective moduli of elastic composites containing randomly dispersed ellipsoidal inhomogeneities. Acta Mech. **103**, 103–121 (1994)
14. Ju, J.W., Chen, T.M.: Effective elastic moduli of two-phase composites containing randomly dispersed spherical inhomogeneities. Acta Mech. **103**, 123–144 (1994)
15. Willis, J.R.: Bounds and self-consistent estimates for the overall properties of anisotropic composites. J. Mech. Phys. Solids **25**, 185–202 (1977)
16. Ju, J.W., Chen, T.M.: Micromechanics and effective elastoplastic behavior of two-phase metal matrix composites. J. Eng. Mater. Technol. ASME **116**, 310–318 (1994)
17. Ju, J.W., Tseng, K.H.: Effective elastoplastic behavior of two-phase ductile matrix composites: A micromechanical framework. Int. J. Solids Struct. **33**(29), 4267–4291 (1996)
18. Ju, J.W., Tseng, K.H.: Effective elastoplastic algorithms for two-phase ductile matrix composites. J. Eng. Mech. ASCE **123**(3), 260–266 (1997)
19. Ju, J.W., Sun, L.Z.: Effective elastoplastic behavior of metal matrix composites containing randomly located aligned spheroidal inhomogeneities. Part I: micromechanics-based formulation. Int. J. Solids Struct. **38**(2), 183–201 (2001)
20. Sun, L.Z., Ju, J.W.: Effective elastoplastic behavior of metal matrix composites containing randomly located aligned spheroidal inhomogeneities. Part II: applications. Int. J. Solids Struct. **38**(2), 203–225 (2001)
21. Ju, J.W., Zhang, X.D.: Micromechanics and effective transverse elastic moduli of composites with randomly located aligned circular fibers. Int. J. Solids Struct. **35**(9–10), 941–960 (1998)
22. Ju, J.W., Zhang, X.D.: Effective elastoplastic behavior of ductile matrix composites containing randomly located aligned circular fibers. Int. J. Solids Struct. **38**(22–23), 4045–4069 (2001)
23. Ju, J.W., Sun, L.Z.: A novel formulation for the exterior-point Eshelby's tensor of an ellipsoidal inclusion. J. Appl. Mech. ASME **66**, 570–574 (1999)
24. Ju, J.W., Lee, H.K.: A micromechanical damage model for effective elastoplastic behavior of ductile matrix composites considering evolutionary complete particle debonding. Comput. Meth. Appl. Mech. Eng. **183**(3–4), 201–222 (2000)

25. Ju, J.W., Lee, H.K.: A micromechanical damage model for effective elastoplastic behavior of partially debonded ductile matrix composites. Int. J. Solids Struct. **38**(36–37), 6307–6332 (2001)
26. Sun, L.Z., Ju, J.W., Liu, H.T.: Elastoplastic modeling of metal matrix composites with evolutionary particle debonding. Mech. Mater. **35**, 559–569 (2003)
27. Sun, L.Z., Liu, H.T., Ju, J.W.: Effect of particle cracking on elastoplastic behavior of metal matrix composites. Int. J. Numer. Meth. Eng. **56**, 2183–2198 (2003)
28. Liu, H.T., Sun, L.Z., Ju, J.W.: An interfacial debonding model for particle-reinforced composites. Int. J. Damage Mech. **13**(2), 163–185 (2004)
29. Sun, L.Z., Ju, J.W.: Elastoplastic modeling of metal matrix composites containing randomly located and oriented spheroidal particles. J. Appl. Mech. ASME **71**, 774–785 (2004)
30. Liu, H.T., Sun, L.Z., Ju, J.W.: Elastoplastic modeling of progressive interfacial debonding for particle-reinforced metal matrix composites. Acta Mech. **181**(1–2), 1–17 (2006)
31. Ju, J.W., Ko, Y.F., Ruan, H.N.: Effective elastoplastic damage mechanics for fiber reinforced composites with evolutionary complete fiber debonding. Int. J. Damage Mech. **15**(3), 237–265 (2006)
32. Lee, H.K., Ju, J.W.: A three-dimensional stress analysis of a penny-shaped crack interacting with a spherical inclusion. Int. J. Damage Mech. **16**(3), 331–359 (2007)
33. Ju, J.W., Oh, S.: Investigation of the crack-dislocation interaction effects. Int. J. Damage Mech. **17**(3), 223–245 (2008)
34. Ju, J.W., Ko, Y.F.: Micromechanical elastoplastic damage modeling for progressive interfacial arc debonding for fiber reinforced composites. Int. J. Damage Mech. **17**(4), 307–356 (2008)
35. Eshelby, J.D.: Elastic inclusions and inhomogeneities. In: Sneddon, I.N., Hill, R. (eds.) Progress in Solid Mechanics. North-Holland, Amsterdam (1961)
36. Mura, T.: Micromechanics of defects in solids, 2nd edn. Kluwer, Dordrecht (1987)
37. Zhao, Y.H., Tandon, G.P., Weng, G.J.: Elastic moduli for a class of porous materials. Acta Mech. **76**, 105–131 (1989)
38. Willis, J.R., Acton, J.R.: The overall elastic moduli of a dilute suspension of spheres. Q. J. Mech. Appl. Math. **29**, 163–177 (1976)
39. Kim, S., Mifflin, R.T.: The resistance and mobility functions of two equal spheres in low-Reynolds-number flow. Phys. Fluids **28**, 2033–2045 (1985)
40. Smith, J.C.: Experimental values for the elastic constants of a particulate-filled glassy polymer. J. Res. NBS **80A**, 45–49 (1976)
41. Walsh, J.B., Brace, W.F., England, A.W.: Effect of porosity on compressibility of glass. J. Am. Ceram. Soc. **48**, 605–608 (1965)